Different components of the RNAi machinery are required for conidiation, ascosporogenesis, virulence, DON production and fungal inhibition by exogenous dsRNA in the Head Blight pathogen *Fusarium graminearum*

Fatima Yousif Gaffar[1†], Jafargholi Imani[1†], Petr Karlovsky[2], Aline Koch[1], Karl-Heinz Kogel[1]

[1] Department of Phytopathology, Centre for BioSystems, Land Use and Nutrition, Justus Liebig University, Heinrich-Buff-Ring 26, D-35392, Giessen, Germany

[2]Department of Crop Sciences, Molecular Phytopathology and Mycotoxin Research, University of Goettingen, D-37077 Goettingen, Germany

Email addresses:

Fatima.Y.Gaffar@agrar.uni-giessen.de

Jafargholi.Imani@agrar.uni-giessen.de

pkarlov@gwdg.de

Aine.Koch@agrar.uni-giessen.de

Karl-Heinz.Kogel@agrar.uni-giessen.de

*Correspondence to Karl-Heinz.Kogel@agrar.uni-giessen.de

† Contributed equally to this work.

Abstract:

Gene silencing through RNA interference (RNAi) shapes many biological processes in filamentous fungi, including pathogenicity. In this study we explored the requirement of key components of fungal RNAi machinery, including DICER-like 1 and 2 (*Fg*DCL1, *Fg*DCL2), ARGONAUTE 1 and 2 (*Fg*AGO1, *Fg*AGO2), AGO-interacting protein *Fg*QIP (QDE2-interacting protein), RecQ helicase (*Fg*QDE3), and four RNA-dependent RNA polymerases (*Fg*RdRP1, *Fg*RdRP2, *Fg*RdRP3, *Fg*RdRP4), in the ascomycete mycotoxin-producing fungal pathogen *Fusarium graminearum* (*Fg*) for sexual and asexual multiplication, pathogenicity, and its sensitivity to double-stranded (ds)RNA. We corroborate and extend earlier findings that conidiation, ascosporogenesis and Fusarium Head Blight (FHB) symptom development require an operable RNAi machinery. The involvement of RNAi in conidiation is dependent on environmental conditions as it is detectable only under low light (< 2 µmol m^{-2} s^{-1}). Although both DCLs and AGOs partially share their functions, the sexual ascosporogenesis is mediated primarily by *Fg*DCL1 and *Fg*AGO2, while *Fg*DCL2 and *Fg*AGO1 contribute to asexual conidia formation and germination. *Fg*DCL1 and *Fg*AGO2 also account for pathogenesis as their knock-out (KO) results in reduced FHB development. Apart from KO mutants *Δdcl2* and *Δago1*, mutants *Δrdrp2*, *Δrdrp3*, *Δrdrp4*, *Δqde3* and *Δqip* are strongly compromised for conidiation, while KO mutations in all *RdPRs, QDE3* and *QIP* strongly affect ascosporogenesis. Analysis of trichothecenes mycotoxins in wheat kernels showed that the relative amount of deoxynivalenol (DON), calculated as [DON] per amount of fungal genomic DNA, was reduced in all spikes infected with RNAi mutants, suggesting the possibility that the fungal RNAi pathways affect *Fg*'s DON production in wheat spikes. Moreover, gene silencing by exogenous target gene specific dsRNA (spray-induced gene silencing, SIGS) is dependent on fungal DCLs, AGOs, and QIP, but not on QDE3. Together these data show that in *F. graminearum* different key components of the RNAi machinery are crucial in different steps of fungal development and pathogenicity.

Introduction:

RNA interference (RNAi) is a conserved mechanism triggered by double-stranded (ds)RNA that mediates resistance to exogenous nucleic acids, regulates the expression of protein-coding genes on the transcriptional and post-transcriptional level and preserves genome stability by transposon silencing (Fire et al., 1998; Mello and Conte , 2004; Hammond, 2005; Baulcombe 2013). Many reports have demonstrated that this natural mechanism for sequence-specific gene silencing also holds promise for experimental biology and offers practical applications in functional genomics, therapeutic intervention, and agriculture (Nowara et al., 2010; Koch and Kogel, 2014; Cai et al., 2018; Zanini et al., 2018). Core RNAi pathway components are conserved in eukaryotes, including most parasitic and beneficial fungi (Cogoni and Macino, 1999; Dang et al., 2011; Carreras-Villaseñor et al., 2013; Torres-Martínez and Ruiz-Vázquez, 2017): DICER-like (DCL) enzymes, which belong to the RNase III superfamily, generate double-stranded small interfering (si)RNAs and micro (mi)RNAs (Meng et al., 2017; Song and Rossi, 2017); ARGONAUTE (AGO) superfamily proteins bind small RNA duplexes to form an RNA-induced silencing complex (RISC) for transcriptional and post-transcriptional gene silencing (PTGS) (Zhang et al., 2015; Nguyen et al., 2018); and RNA-dependent RNA polymerases (RdRPs) are involved in the production of dsRNA that initiate the silencing mechanism as well as in the amplification of the silencing signals through the generation of secondary siRNAs (Calo et al., 2012).

Fungal RNAi pathways contribute to genome protection (Meng et al., 2017), pathogenicity (Weiberg et al., 2013; Kusch et al., 2018; Zanini et al. 2019), development (Carreras-Villaseñor et al., 2013), and antiviral defense (Segers et al., 2007; Campo et al., 2016; Wang et al., 2016a). In *Aspergillus flavus* (Bai et al., 2015), *Magnaporthe oryzae* (Raman et al., 2017) and *Penicillium marneffei* (Lau et al., 2013), sRNAs were shown to be responsive to environmental stress. In *Trichoderma atroviride*, both light-dependent asexual reproduction and light-independent hyphal growth require an operational RNAi machinery (Carreras-Villaseñor et al., 2013). Similarly, in *Mucor circinelloides*, defects in the RNAi machinery resulted in various developmental defects such as dysfunction during sexual and asexual reproduction (Torres-Martínez and Ruiz-Vázquez, 2017).

Neurospora crassa, a model organism for studying RNAi in filamentous fungi, has different silencing pathways, including quelling (Romano et al., 1992) and meiotic silencing by unpaired DNA (MSUD) (Shiu et al., 2001). In the vegetative stage, the introduction of transgenes results in PTGS of the transgenes and cognate endogenous mRNAs, an RNAi silencing phenomenon known as quelling. The process requires *QDE3* (*Quelling defective 3*), which encodes a RecQ

helicase, and RPA (subunit of replication protein A), which recognizes aberrant DNA structures. Interaction of these proteins recruits Quelling defective 1 (QDE1), a protein with dual function as DNA-dependent RNA polymerase (DdRP) and RdPR, to the single-stranded (ss)DNA locus, resulting in production of aberrant ssRNAs and its conversion to dsRNAs. Subsequently the dsRNA is processed into small RNAs by DCL1. sRNAs duplexes are loaded onto QDE2 (Quelling defective 2), which encodes an AGO homolog. QDE2 cleaves the passenger strand and the exonuclease QIP (QDE2-interacting protein) assists to remove it to form an active RISC that targets complementary mRNA for degradation (Chang et al., 2012). MSUD occurs during sexual development in prophase I of meiosis, when unpaired homologous DNA sequences have been detected during the pairing of the homologous chromosomes, which then also leads to the production of aberrant RNA transcripts (Chang et al., 2012). Genes required for MSUD are *SAD1* (*Suppressor of ascus dominance 1*), a paralog of QDE-1, and SAD2. SAD2 recruits SAD1 to the perinuclear region, where aberrant RNA is converted to dsRNA. Upon silencing by DCL1, the small RNA duplexes are loaded onto SMS2 (Suppressor of meiotic silencing 2), an AGO homolog in *Neurospora*, which also is assisted by QIP. In contrast, QDE-2 and DCL2 are not required for MSUD in *Neurospora* , indicating that there are two parallel RNAi pathways functioning separately in the vegetative and meiotic stages.

Fusarium graminearum (*Fg*) is one of the devastating pathogens of cereals causing Fusarium Head Blight (FHB) and Crown Rot (FCR) (Dean et al., 2012; Harris et al., 2016). The pathogen belongs to the filamentous ascomycetes. Ascospores are the primary inoculum for FHB epidemics as these spores are forcibly shot into the environment and also can pass long distances (Maldonado-Ramirez et al., 2005). Moreover, the sexual development ensures the formation of survival structures necessary for overwintering (Dill-Macky and Jones, 2000) and the genetic diversity of the population (Cuomo et al. 2007). Of note, spike infections can be symptomless or symptomatic (Urban et al., 2015; Brown et al., 2017). In both cases, *Fusarium* fungi contaminate the grain with mycotoxins and thus decrease grain quality. Among the mycotoxins, the B group trichothecenes, including deoxynivalenol (DON), nivalenol (NIV), and their acetylated derivatives (3A-DON, 15A-DON, and 4A-NIV) influence the virulence of the fungus (Ilgen et al., 2009; Desjardins et al., 1993; Jansen et al., 2005). Mycotoxins such as DON trigger an oxidative burst in the host plants, resulting in cell necrosis and disintegration of the defense system, which then favors colonization of the plant tissues by a necrotrophic fungus (Audenaert et al., 2014). Importantly, *Fg* possesses a functional MSUD mechanism (Son et al., 2011) and *AGO* genes *FgSMS2* or *FgAGO2* are necessary for sexual reproduction (Kim et al., 2015). A recent work discovered that the sex-induced RNAi mechanism has important

roles in sexual reproduction (Son et al., 2017). siRNAs produced from exonic gene regions (ex-siRNAs) participate in PTGS at a genome-wide level in the late stages of sexual reproduction. The sex-specific RNAi pathway is primarily governed by *Fg*DCL1 and *Fg*AGO2. Thus, *Fg* primarily utilizes ex-siRNA-mediated RNAi for ascospore formation. Consistent with the key role of *Fg*DCL1 in generative development, the combination of sRNA and transcriptome sequencing predicted 143 novel microRNA-like RNAs (milRNAs) in wild-type perithecia, of which most were depended on *Fg*DCL1. Given that 117 potential target genes were predicted, these perithecium-specific milRNAs may play roles in sexual development (Zeng et al., 2018). To develop RNAi-based plant protection strategies such as host-induced gene silencing (HIGS) (Koch et al. 2013) and spray-induced gene silencing (SIGS) (Koch et al., 2016; Koch et al. 2018) against *Fusarium* species, it is required to bank on knowledge about the RNAi components involved in *Fusarium* development and pathogenicity. A report of Chen and colleagues (Chen et al., 2015) demonstrated that, in *Fg*, a hairpin RNA (hpRNA) can efficiently silence the expression level of a target gene, and that the RNAi components *Fg*DCL2 and *Fg*AGO1 are required for silencing. This finding is consistent with reports showing that a *Fg* wild-type (wt) strain, but not *Fg* RNAi mutants, are amenable to SIGS-mediated target gene silencing, when it grows on a plant sprayed with exogenous dsRNA directed against the fungal *Cytochrome P450 lanosterol C-14α-demethylase* (*CYP51*) genes (Koch et al., 2016). In this study, we expanded previous studies to address the requirement of an extended set of *Fg* RNAi genes in growth, reproduction, virulence, toxin production, and SIGS-mediated inhibition of fungal infection of barley leaves.

Results:

Requirement of RNAi pathway core components under different light regimes

The *Fg* genome obtained from the Broad Institute (www.broadinstitute.org) contains many functional RNAi machinery components (Chen et al., 2015; Son et al., 2017). We generated *Fg* gene replacement mutants for several major RNAi genes by homolog recombination using the pPK2 binary vector (**Table 1**). Disruption vectors for *FgDCL1*, *FgDCL2*, *FgAGO1*, *FgAGO2*, *FgRdRP1*, *FgRdRP2*, *FgRdRP3*, *FgRdRP4*, *FgQDE3*, and *FgQIP* were constructed by inserting two flanking fragments (~1000 bp) upstream and downstream of the corresponding genes in pPK2 vector (**Table S1**; **Figure S1**). The vectors were introduced into *Agrobacterium tumefaciens*, followed by agro-transformation of the *Fg* strain IFA. Transformants were transferred to Petri dishes of potato extract glucose (PEG) medium, containing 150 µg/ml hygromycin and 150 µg/ml ticarcillin. Mutants were verified by PCR analysis with genomic DNA as template (**Figure 1**) and by expression analysis of the respective RNAi gene (Fig. S2). Colony morphology of PCR verified mutants (12h/12h light/dark, see methods) was inspected in axenic cultures of three different media, PEG, synthetic nutrient (SN) agar and starch agar (SA). In the PEG agar medium, all mutants showed slightly reduced radial growth, while there were no clear differences as compared with the IFA wild type (WT) WT strain in SN and SA media (**Figures S3 A-C**). In liquid PEG medium under day light conditions, all mutants produced comparable amounts of mycelium biomass, though different amounts of the red pigment aurofusarin (Frandsen et al., 2006): *Δdcl1*, *Δdcl2*, *Δrdrp1*, *Δqde3,* and *Δqip1* showed reduced pigmentation, while *Δago1*, *Δrdrp2*, *Δrdrp3*, and *Δrdrp4* showed higher pigmentation compared to IFA WT (**Figure S3 D**; **Table 2**). Under light induction conditions (12 h light; 52 µmol m^{-2} s^{-1}), conidia grown in 96-well-plate liquid SN cultures showed normal germ tube emergence (not shown). All RNAi mutants formed an elongated hyphal cell type, producing abundant conidia on conidiophores and directly from hyphae. Conidia were moderately curved with clear septations.

When grown continuously under dimmed light (2 µmol m^{-2} s^{-1}), liquid SN cultures of RNAi mutants showed significantly reduced conidiation compared to IFA WT, except *Δago2* and *Δrdrp1*, which were only slightly affected (**Figure 2 A**). Under this non-inductive condition, some RNAi mutants also were compromised in conidial germination: *Δago1*, *Δago2* and *Δrdrp4* showed significantly reduced germination, while *Δrdrp3*, *Δdcl1*, *Δrdrp1* and *Δdcl2* showed a slight reduction, and *rdrp2*, *Δqip* and *Δqde3* showed normal conidial germination (**Figure 2 B**; see **Table 2**). All RNAi mutants had a normal germ tube morphology, except *Δrdrp4*, which tends to develop multiple germ tubes (**Figure 2 C**). These results suggest a requirement for *Fg*

RNAi components genes in the full control of asexual development depending on the environmental conditions.

F. graminearum RNAi components are required for sexual development

Because there were contrasting data in the literature, we resumed asking the question of whether RNAi components are required for sexual reproduction of *Fg*. Perithecia (fruiting bodies) formation was induced in axenic cultures on carrot agar (Cavinder et al., 2012). All RNAi mutants produced melanized mature perithecia to the same extend as compared to IFA WT (not shown). Next, we assessed the forcible discharge of ascospores by a spore discharge assay (**Figure 3**). Discharge of ascospores from perithecia into the environment results from turgor pressure within the asci; the dispersal of ascospores by forcible discharge is a proxy for fungal fitness as it is important for dissemination of the disease. To this end, half circular agar blocks covered with mature perithecia were placed on glass slides and images from forcibly fired ascospores (white cloudy) were taken after 48 h incubation in boxes under high humidity and fluorescent light. We found that the forcible discharge of ascospores was severely compromised in *Δdcl1*, *Δago2*, *Δrdrp1*, *Δrdrp2*, *Δqde3*, and less severe in *Δdcl2*, *Δago1*, *Δqip1*, while *Δrdrp3* and *Δrdrp4* were indistinguishable from IFA WT. (**Figures 3 A, B**). Microscopic observation of the discharged ascospores revealed that their morphology was not affected (not shown). However, the percentage of discharged ascospores that retained the ability to germinate varied in the mutants with *Δrdrp3* and *Δrdrp4*, showing strong reduction in the ascospore germination (**Figure 3 C**; see **Table 2**). Together, these results confirm that the RNAi pathway is involved in sexual reproduction, though the requirement of individual RNAi components greatly varies in the different developmental stages.

F. graminearum RNAi mutants show variation in kernel infection

It has been reported that *Fg* mutants defective in DCL, AGO, or RdRP were not compromised in virulence on wheat spikes (Chen et al., 2015). We extended this previous study by testing additional *Fg* RNAi mutants. Conidia were point-inoculated to a single spikelet at the bottom of a spike of the susceptible wheat cultivar Apogee. Fungal colonization was quantified nine and 13 days post inoculation (dpi) by determining the infection strength. Infected parts of a spike bleached out, whereas the non-inoculated spikes remained greenish. At late infection stages (13 dpi), all RNAi mutants caused strong FHB symptoms comparable with IFA WT. However, we found clear differences in the severity of infections at earlier time points (9 dpi), with *Δdcl1* and *Δago2* showing most compromised FHB development (**Figure** 4 A; see **Table**

2). At 13 dpi, RNAi mutants also showed considerable variation on *Fg*-infected kernel morphology (**Figure S4 A**). Thousand-grain-weight (TGW) of kernels infected with RNAi mutants showed slight, though not significant differences, in the total weights compared to IFA WT infection (**Figure S4 B**).

DON production is compromised in *F. graminearum* mutants that show reduced pathogenicity on wheat kernels

We quantified the amount of DON in *Fg*-infected wheat spikes at 13 dpi (point-inoculation using 5 µl of 0.002% Tween 20 water containing 40,000 conidia / mL) at mid-anthesis. Of note, the relative amount of DON [rDON], calculated as [DON] relative to the amount of fungal genomic DNA, was reduced in virtually all spikes infected with RNAi mutants, whereby spikes infected by *Δqip* and *Δdcl2* showed the lowest toxin reduction as compared with the other mutants (**Table 3**). The data suggest that fungal RNAi pathways affect *Fg*'s DON production in wheat spikes. While [rDON] changed, the ratio of [DON] and [A-DON] (comprising 3A-DON and 15A-DON) remained constant in all mutants vs. IFA WT, suggesting that the fungal RNAi pathways do not affect the trichothecene metabolism.

F. graminearum RecQ helicase mutant *Δqde3* is insensitive to dsRNA

Spraying plant leaves or fruits with dsRNA targeting essential fungal genes can reduced fungal infections by spray-induced gene silencing (SIGS) (Koch et al., 2016; Wang et al., 2016b; Dalakouras et al., 2016; McLoughlin et al., 2018). We addressed the question which RNAi mutants are compromised in SIGS upon treatment with dsRNA. To this end, we conducted a SIGS experiment on detached barley leaves that were sprayed with 20 ng μL^{-1} CYP3RNA, a 791 nt long dsRNA that targets the three fungal genes *FgCYP51A*, *FgCYP51B* and *FgCYP51C* (Koch et al., 2016). By 48 h after spraying, leaves were drop inoculated with 5 x 10^4 conidia ml^{-1} of *Fg* RNAi mutants and IFA WT. Five days later, infected leaves were scored for disease symptoms and harvested to measure the expression of the fungal target genes by qPCR (**Figure 5**). As revealed by reduced disease symptoms, leaves sprayed with CYP3RNA vs. TE (buffer control), only *Δqde3* was equally sensitive to dsRNA like the IFA WT, while all other mutants tested in this experiment were slightly or strongly compromised in SIGS and less sensitive to CYP3RNA (**Figure 5 A**, see **Table 2**). Consistent with this, strong down-regulation of all three *CYP51* target genes was observed only in IFA WT and *Δqde3*. In *Δdcl1*, *Δdcl2* and *Δqip1*, the inhibitory effect of CYP3RNA on *FgCYP51A*, *FgCYP51B* and *FgCYP51C* expression was completely abolished (**Figure 5B**). To further substantiate this finding, we tested a *dcl1/dcl2* double mutant in *Fg* strain PH1. As anticipated from the

243 experiments with IFA WT, the PH1 *dcl1/dcl2* mutant was fully compromised in SIGS (**Figures**
244 **5A, B**).
245

Discussion

We generated a broad collection of knock-out mutants for RNAi genes in the necrotrophic, mycotoxin-producing pathogen *Fusarium graminearum* to demonstrate their involvement in vegetative and generative growth, disease development, mycotoxin production, and sensitivity to environmental RNAi. A summary of the mutants' performance in the various processes is shown in Table 2. While all RNAi mutants show normal vegetative development in axenic cultures, there were differences in pigments production in liquid potato extract glucose cultures. This suggests that in *Fg* an RNAi pathway regulates the gene cluster responsible for the biosynthesis of pigments, including aurofusarin. Aurofusarin is a secondary metabolite belonging to the naphthoquinone group of polyketides that shows antibiotic properties against filamentous fungi and yeast (Medentsev et al., 1993). The function of the compound in the fungus is unknown as white mutants have a higher growth rate than the wt and are as pathogenic on wheat and barley (Malz et al., 2005).

Overall, the contribution of the RNAi pathways to vegetative fungal development and conidiation varies among different fungi and must be considered case by case. Under low light (< 2 µmol m^{-2} s^{-1}) all *Fg* RNAi mutants showed reduced conidia production and some showed aberrant germination compared to IFA WT. This suggests that in the absence of light induction the RNAi pathway is required for conidiation. RNAi may play a role in regulation of light responsive genes affecting conidiation as shown for *T. atroviride*, where DCL2 and RdRP3 control conidia production under light induction (Carreras-Villaseñor et al., 2013). The authors claimed that *Δdcl2* and *Δrdrp3* are impaired in perception and/or transduction of the light signal affecting the transcriptional response of light-responsive genes. Similarly, *Metarhizium robertsii dcl* and *ago* mutants show reduced abilities to produce conidia under light, though the light quantity was not described (Meng et al., 2017).

Perithecia development has been used to study sexual development and transcription of genes related to sexual development (Trail et al., 2000; Qi et al., 2006; Hallen et al., 2007). In field situations, ascospores serve as the primary inoculum for FHB epidemics because these spores are shot into the environment and can spread long distances (Maldonado-Ramirez et al., 2005). We found that all RNAi mutants could produce mature perithecia. However, corroborating and extending the exemplary work of Son et al. (2017), we also found that, beside *FgDCL1* and *FgAGO2*, other RNAi genes such as *RdRP1*, *RdRP2*, *RdRP3*, *RdRP4*, *QDE3*, *QIP* contribute to the sexual reproduction. Mutations in these genes either showed severe defect in forcible ascospore discharge or significantly reduced germination. The Son et al. (2017) study showed

that *Fgdcl1* and *Fgago2* are severely defective in forcible ascospore discharge, while *Fgdcl2* and *Fgago1* show indistinguishable phenotypes compared to the wt. Active roles for *Fg*DCL1 and *Fg*AGO2 is supported by the finding that expression levels of many genes, including those closely related to the mating-type (*MAT*)-mediated regulatory mechanism during the late stages of sexual development, was compromised in the respective mutants after sexual induction (Kim et al., 2015). Moreover, *Fg*DCL1 and *Fg*AGO2 participate in the biogenesis of sRNAs and perithecia-specific miRNA-like RNAs (milRNAs) also are dependent on *Fg*DCL1 (Zeng et al., 2018). Most of the produced sRNA originated from gene transcript regions and affected expression of the corresponding genes at a post-transcriptional level (Son et al., 2017).

While our data show that, in addition to *Fg*DCL1 and *Fg*AGO2, more *Fg* RNAi-related proteins are required for sex-specific RNAi, further transcriptomic analysis and sRNA characterization are needed for a mechanistic explanation. Of note, ex-siRNA functions are important for various developmental stages and stress responses in the fungus *M. circinelloides*, while *Fg* utilizes ex-siRNAs for a specific developmental stage. Thus, ex-siRNA-mediated RNAi might occur in various fungal developmental stages and stress responses depending on the fungal species.

We investigated the involvement of RNAi in pathogenicity and FHB development by infecting wheat spikes of the susceptible cultivar Apogee with fungal conidia. At earlier time points of infection (9 dpi) clear differences in virulence between RNAi mutants were observed, though all mutants could spread within a spike and caused typical FHB symptoms at later time points (13 dpi). Despite full FHB symptom development in all mutants at 13 dpi, we observed various effects of fungal infection on the kernel morphology, corresponding to the different aggressiveness of mutants at early time points. Since this phenomenon may account for differences in producing mycotoxins during infection, we quantified mycotoxins in the kernels. Of note, [rDON] was reduced in virtually all spikes infected with RNAi mutants, whereby [rDON] was strongly reduced especially in spikes colonized with mutants *Δago1*, *Δrdrp1*, *Δrdrp2*, *Δrdrp3*, *Δrdrp4* and *Δqde3* as compared with IFA WT (see Table 2 and Table 3). The data suggest that fungal RNAi pathways affect *Fg*'s DON production in wheat spikes. While [rDON] changed, the ratio of [DON] and [3A-DON] remained constant in all mutants vs. IFA WT, suggesting that the fungal RNAi pathways do not affect the trichothecene chemotype.

Our work also identifies additional *Fg* RNAi proteins associated with sensitivity to dsRNA treatments. For the validation of the effects we used two independent tests: infecting phenotyping and qRT-PCR analysis of fungal target genes. *Δdcl1* and *Δdcl2* as well as *Δqip* and *Δrdrp* showed compromised SIGS phenotypes in either tests, strongly suggesting that these

314 proteins are required for environmental RNAi in *Fg*. Further substantiating our finding, the
315 fungal *dcl1/dcl2* double mutant of *Fg* strain PH1 also showed complete insensitivity to dsRNA
316 and thus is fully compromised to environmental RNAi.
317 Taken together, our results further substantiate the involvement of RNAi pathways in
318 conidiation, ascosporogenesis and pathogenicity of *Fg*. Nevertheless, further studies must
319 explore the mechanistic roles of *Fg* RNAi genes in these processes.
320

Methods:

Fungal material, generation of gene deletion mutants in *Fusarium graminearum*

The *Fg* strain PH1 and the PH1 *dcl1 dcl2* double mutant were a gift of Dr. Martin Urban, Rothamsted Research, England. RNAi gene deletion mutants were generated in the *Fg* strain IFA65 (Jansen et al. 2005) hereafter termed IFA WT. They were generated by homolog recombination using the pPK2 binary vector. *Fg* RNAi genes were identified by blasting *Neurospora crassa* genes against the Fusarium genome sequence in the Broad institute data base. Disruption vectors were constructed by inserting two flanking fragments (~1000 bp) upstream and downstream the corresponding genes in the pPK2 vector as follows: *RdRP1*, *AGO1*, *QDE3*, *QIP*, *AGO2*, *DCL1*, *RdRP2*, *RdRP3*, *RdRP4* and *DCL2* upstream flanking sequences were inserted in the plasmid between PacI- KpnI restriction sites, and the downstream flanking sequence were inserted between XbaI- HindIII restriction sites. Except *AGO2* downstream flanking sequence was inserted in XbaI restriction site (primers used in disruption plasmid construction are listed in Table S1. Disruption vectors were introduced into *Agrobacterium tumefaciens* (LBA440 and AGL1 strains) by electroporation. A single colony of Agrobacterium containing the pPK2 plasmid were grown in 10 ml YEB medium (Vervliet et al., 1975) containing the appropriate antibiotics (5 µg/ml tetracicllin + 25 µg/ml rifampicin + 50 µg/ml Kanamycin for LBA440, and 25 µg/ml carbenicillin + 25 µg/ml rifampicin + 50 µg/ml kanamycin for AGL1) and were incubated at 28ºC till OD_{600nm} 0.7 was reached. T-DNA was mobilized in Agrobacterium with 200 µM acetosyringone, and Agrobacterium and fungal recipient IFA WT were co-cultivated on black filter paper (DP 551070, Albert LabScience, Hahnemühle, Dassel, Germany), respectively. Putative fungal mutants were selected on potato extract glucose (PEG) medium containing 150 µg/ml hygromycin + 150 µg/ml ticarcillin and grown for five days. For genotyping, genomic DNA of putative Fusarium mutants were extracted from mycelia.

Genotyping of Fusarium mutants

Fg IFA mutants were confirmed by genotyping using primers located in hygromycin and corresponding gene flanking sequences (located after the cloned flanking sequence in the genome) (Table S2). Upon amplification the samples were sequenced. Additionally, mRNA expression levels of deleted vs. levels in IFA WT was measured by quantitative real time PCR (qRT-PCR) using primers pairs listed in (Table S3). The mRNA transcripts were measured using 1 x SYBR Green JumpStart Taq Ready Mix (Sigma-Aldrich, Germany) according to

355 manufacturer's instructions and assayed in 7500 Fast Real-Time PCR cycler (Applied
356 Biosystems Inc, CA, USA) under the following thermal cycling conditions: initial activation
357 step at 95°C for 5 min, 40 cycles (95°C for 30 s, 53°C for 30 s, and 72°C for 30 s). The Ct
358 values were determined with the software in the qRT-PCR instrument and the transcript levels
359 of the genes was determined according to the $2^{-\Delta\Delta Ct}$ method (Livak and Schittgen, 2001).
360
361 **Colony morphology**
362 The RNAi mutants were cultured on PEG (ROTH, Germany); starch agar (SA) and synthetic
363 nutrient agar (SNA) (Leslie and Summerell, 2006). The cultures were incubated at 25ºC in 12
364 h light/12 h dark (52 µmol m^{-2} s^{-1}, Philips Master TL-D HF 16W/840). The growth was
365 documented after 5 days. For growth in liquid cultures, agar blocks from two-week-old fungal
366 cultures were incubated on liquid PEG medium for five days at room temperature (RT), light
367 (2 µmol m^{-2} s^{-1}) with shaking. Each mutant was grown in flask containing medium
368 supplemented with hygromycin (100 µg/ml) and flask containing medium without hygromycin.
369 Photos were taken to document the growth pattern after five days incubation.
370
371 **Production of fungal biomass**
372 Fifty milligram mycelia (fresh mycelia from four-day-old fungal cultures grown on Aspergillus
373 complete medium (CM) plates in the dark; Leslie and Summerell, 2006) were incubated in a
374 100 ml flask containing 20 ml of PEG medium incubated at RT with shaking under 12 h light
375 (2 µmol m^{-2} s^{-1}). Fungal mycelium was harvested after three days by filtration through filter
376 paper (Munktell, AHLSTROM, Germany GMBH), washed with distilled water twice and dried
377 at 75°C overnight. The dry weight was calculated by using the following formula: Dry weight
378 = (weight of filter paper + mycelium) - (weight of filter paper).
379
380 **Conidiation assay**
381 Production of conidia was done according to Yun et al., (2015) with slight modification. Four-
382 day-old cultures of each mutant and IFA WT growing in CM agar plates in the dark at 25°C
383 were used for fresh mycelia preparation. The mycelia were scraped from the plate surface using
384 a sterile toothpick, then 50 mg mycelia were inoculated in a 100 ml flask containing 20 ml of
385 SN medium. The flasks were incubated at RT for five days in light (2 µmol m^{-2} s^{-1}) on a shaker
386 (100 rpm). Subsequently, the conidia produced from each mutant and wt were counted using a
387 hemocytometer (Fuchs Rosenthal, Superior Marienfeld, Germany).
388

Viability test of conidia

Fourteen mL from the same cultures used in conidiation assay were centrifuged at 4,000 rpm for 10 min to precipitate conidia. The conidia were resuspended in 5 ml 2% sucrose water and incubated in dark for two days at 23°C. Germinated and non-germinated conidia were visualized and counted under an inverse microscope. Conidia germination rate was determined as percentage of germinated conidia of the total conidia number.

Perithecia production and ascospore discharge assay

Fungi were grown on carrot agar prepared under bright fluorescent light at RT (18-24°C) for five days (Klittich and Leslie, 1988). Aerial mycelia were removed with a sterile tooth stick. To stimulate sexual reproduction and perithecia formation, one ml of 2.5% Tween 60 was applied to the plates with a sterile glass rod after scraping the mycelia (Cavinder et al., 2012). The plates were incubated under fluorescent light at RT for nine days. Subsequently, agar blocks (1.5 cm in diameter) were cut from the plates containing the mature perithecia using a cork borer. Agar blocks were sliced in half, placed on glass microscope slides, and incubated in boxes under high humidity for two days under 24 h light (52 µmol m^{-2} s^{-1} Philips Master TL-D HF 16W/840). During this time, ascospores discharged from the perithecia accumulated on the slide. For the quantification of discharged ascospores, slides were washed off by 2 ml of an aqueous Tween 20 (0.002%) solution and counted using a hemocytometer.

Viability test of the discharged ascospores

Mycelia with mature perithecia (13 days after sexual induction) on carrot agar were incubated in a humid box at RT under light for four days according to Son et al., (2017). The discharged ascospores were washed from the plate cover using SN liquid medium and incubated in the dark for 24 h in a humid box. The germinated and non-germinated ascospores were visualized under an inverse microscope and counted.

Pathogenicity assay on wheat ears

The susceptible wheat cultivar Apogee was used. Plants were grown in an environmentally controlled growth chamber (24°C, 16 h light, 180 µmol m^{-2} s^{-1} photon flux density, 60% rel. humidity) till anthesis. Point inoculations to the second single floret of each spike were performed at mid-anthesis with 5 µL of a 40,000 conidia/mL suspension amended with 0.002% v/v Tween 20 (Gosman et al., 2010). Control plants were treated with sterile Tween 20. For each *Fg* genotype, ten wheat heads were inoculated and incubated in plastic boxes misted with

water to maintain high humidity for two days. Incubation continued at 22°C in 60% rel. humidity. Infected wheat heads were observed nine and 13 dpi and infection percentage was determined as the ratio of infected spikelets to the total spikelet number per ear.

Thousand Grain Weight (TGW) of infected wheat kernels

A hundred kernels from two biological experiments with 10 wheat heads point-inoculated with IFA WT and mutants were counted and weighed. TGW was calculated in grams per 1000 kernels of cleaned wheat seeds.

Quantification of fungal DNA in infected wheat kernels

Fungal genomic DNA in kernels was quantified using qPCR as described (Brandfass and Karlovsky, 2008). Dried grains were ground and DNA was extracted from 30 mg flour and dissolved in 50 µl of TE buffer. One µl of 50x diluted DNA was used as template for RT-PCR with primers amplifying a 280 bp fragment specific for *Fg*. The PCR mix consisted of reaction buffer (16 mM $(NH_4)_2SO_4$, 67 mM Tris–HCl, 0.01% Tween-20, pH 8.8 at 25°C; 3 mM $MgCl_2$, 0.3 µM of each primer, 0.2 mM of each dATP, dTTP, dCTP and dGTP (Bioline), 0.03 U/µl Taq DNA polymerase (Bioline, Luckenwalde, Germany) and 0.1x SYBR Green I solution (Invitrogen, Karlsruhe, Germany). The PCR was performed in CFX384 thermocycler (BioRad, Hercules, CA, USA) according to the following cycling condition: Initial denaturation 2 min at 95°C, 35 cycles with 30 s at 94°C, 30 s at 61°C, 30 s at 68°C, and final elongation for 5 min at 68°C. No matrix effects were detectable with 50-fold diluted DNA extracted from grains. Standards were prepared from pure *Fg* DNA in 3-fold dilution steps from 100 pg to 0.4 pg/well.

Analysis of mycotoxins in infected wheat kernels

The content of mycotoxins in wheat kernels infected with *Fg* RNAi mutants and IFA WT was determined using high performance liquid chromatography coupled to tandem mass spectrometry (HPLC–MS/MS). Mycotoxins were extracted from ground grains with mixture containing 84% acetonitrile, 15% water and 1% acetic acid and the extracts were defatted with cyclohexane. Chromatographic separation was carried out on a C18 column eluted with a water/methanol gradient and the analytes were ionized by electrospray and detected by MS/MS in multiple reaction monitoring (MRM) mode essentially as described (Sulyok et al., 2006).

Spray application of dsRNA on barley leaves

Second leaves of three-week-old barley cultivar Golden Promise were detached and transferred to square Petri plates containing 1% water-agar. dsRNA spray applications and leaf inoculation was done as described (Koch et al. 2016). For the TE-control, TE-buffer was diluted in 500 µl water corresponding to the amount used for dilution of the dsRNA. Typical RNA concentration after elution was 500 ng μl^{-1}, representing a buffer concentration of 400 µM Tris-HCL and 40 µM EDTA in the final dilution. TE buffer were indistinguishable from treatments with control dsRNA generated from the GFP or GUS gene, respectively (Koch et al., 2016; Koch et al., 2018). Thus, we used TE buffer as control to save costs. Spraying of the leaves was carried out in the semi-systemic design (Koch et al. 2016), where the lower parts of the detached leaf segments were covered by a tinfoil to avoid direct contact of dsRNA with the leaf surface that was subsequently inoculated.

Statistics and analysis

Data obtained from two or three repetitions were subjected to the Student's *t* test in Microsoft office Excel 2010. Significance was determined as $P \leq 0.05$, 0.01 or 0.001 and indicated by *, ** or ***, respectively. Unless specified otherwise, data are presented as mean ± standard error or mean ± standard deviation of the mean. Sequence analysis was performed on the ApE plasmid editor free tool. Basic Local Alignment Search Tool (BLAST) NCBI BLAST (http://blast.ncbi.nlm.nih.gov/Blast.cgi) was used for sequences search and alignment.

List of abbreviations

AGO, ARGONAUTE

CYP51, *Cytochrome P450 lanosterol C-14α-demethylase*

DCL, DICER-like

DON, deoxynivalenol

Fg, *Fusarium graminearum*

FHB, Fusarium head blight

HIGS, host-induced gene silencing

hpRNA, hairpin RNA

MSUD, meiotic silencing by unpaired DNA

NIV, nivalenol

PEG, potato extract glucose

QDE 2,3, Quelling defective 2,3

490 QIP, QDE-interacting protein
491 RdRp, RNA-dependent RNA polymerase
492 RISC, RNA-dependent silencing complex
493 RNAi, RNA interference
494 RPA, subunit of replication protein A
495 siRNA, small interfering RNA
496 SN, synthetic nutrient agar
497 ssDNA, single-stranded
498 TGW, thousand grain weight
499

500 **Declarations**

501 **Ethics approval and consent to participate**
502 Not applicable
503 **Consent for publication**
504 Not applicable

505 **Availability of data and material**
506 All data generated or analysed during this study are included in this published article [and its
507 supplementary information files].

508 **Competing interests**
509 The authors declare that they have no competing interests" in this section.
510

511 **Funding**
512 This research was supported by the German Research Council (DFG) to K.-H. K and AK in the
513 project GRK2355.
514

515 **Acknowledgements**
516 We thank Mrs. E. Stein for excellent technical assistance, Dr. A. Rathgeb for mycotoxin
517 analysis and Ms. C. Birkenstock for caring of the plants. We also thank Dr. Martin Urban,
518 Rothamsted Research, England for providing the *Fg* strains PH1 and PH1 *dcl1 dcl2*.

519 **Legends to figures**

520

521 **Fig. 1. PCR verification of targeted gene replacement in *Fusarium graminearum*. (A)**
522 Amplification of an internal part of the targeted genes *DCL1*, *DCL2*, *AGO1*, *AGO2*, *RdRP1*,
523 *RdRP4*, *RdRP2*, *RdRP3*, *QIP*, and *QDE3* are positive in IFA WT and negative in corresponding
524 mutants. (**B)** PCR with primer pairs in the right recombination sequence and hygromycin,
525 showing that the antibiotic resistance gene had integrated into the target gene locus. PCR
526 products were analyzed on 1.5% agarose gel electrophoresis. M; DNA marker. wt; wild type.

527

528 **Fig. 2. The RNAi pathway is required for asexual development of *Fusarium graminearum***
529 **in the absence of inductive light. (A)** Number of conidia produced: Means± SEs of the
530 percentage of conidia numbers from three repeated experiments. Significant differences are
531 marked: *P, 0.05, **P, 0.01, ***P, 0.001 (Student's *t* test). **(B)** Percent of conidial germination:
532 Means± SEs of the percentage of germinated spores from three biological repetitions.
533 Significant differences are marked: *P, 0.05 (Student's t test). **(C)** Microscopic observation of
534 germinated and non-germinated conidia of IFA WT and *Δrdrp4*. Imaging after 48 h incubation
535 in the dark, scale bar: 50 µm. Black arrow; conidia forming a bipolar germ tube. Red arrow;
536 conidia forming multiple germ tubes.

537

538 **Fig. 3. Forcible ascospore discharge in *Fusarium graminearum* RNAi mutants and IFA**
539 **WT. (A)** Forcible ascospore firing. Half circular carrot agar blocks covered with mature
540 perithecia were placed on glass slides. Photos from forcibly fired ascospores (white cloudy)
541 were taken after 48 h incubation in boxes under high humidity and fluorescent light. **(B)** Fired
542 ascospores were washed off and counted. Means± SDs of the counted spores is presented from
543 three biological repetitions. Significant differences are marked: *P, 0.05, ***P, 0.001
544 (Student's t test). **(C)** Ascospore germination. Discharged ascospores were incubated at 100%
545 RT in the dark for 24 h at 23°C in SN liquid medium. The percentage of germination was
546 assessed by examining the ascospore number in three random squares in the counting chamber.
547 Means± SEs of the percentage of germinated spores from three biological repetitions.
548 Significant differences are marked: *P, 0.05 (Student's t test).

549

550 **Fig. 4. Infection of Apogee wheat spikes with *Fusarium graminearum* RNAi mutants and**
551 **IFA WT. (A)** Representative samples of spikes at 9 and 13 dpi. One spikelet at the bottom of
552 each spike (red arrow) was point inoculated with 5 µl of 0.002% Tween 20 water containing

40,000 conidia / mL. The assay was repeated two times with 10 spikes per fungal genotype and experiment. **(B)** Wheat kernels 13 dpi with *Fg* RNAi mutants and IFA WT.

Fig. 5 Infection symptoms of *Fg* RNAi mutants on barley leaves sprayed with the dsRNA CYP3RNA. **A.** Detached leaves of three-week-old barley plants were sprayed with 20 ng μl^{-1} CYP3RNA or TE buffer, respectively. After 48 h, leaves were drop-inoculated with 5 x 10^4 conidia ml^{-1} of indicated *Fg* RNAi mutants and evaluated for infection symptoms at 5 dpi. Values show relative infection area as calculated from TE- vs. CYP3RNA-treated plants for each RNAi mutant with 10 leaves and thee biological repetitions. Asterisks indicate statistical significant reduction of the infection area on CYP3RNA- vs. TE-treated plants measured by ImageJ for each mutant (**p<0,01; ***p< 0,001; students t-test). The *dcl1 dcl2* double mutant is generated in *Fg* strain PH1. (**B**). Downregulation of the three *CYP51* genes in *Fg* mutants upon colonization of CYP3RNA- vs. TE-treated barley leaves. Asterisks indicate statistical significant downregulation of *CYP51* genes on CYP3RNA vs. TE-treated plants. (**p<0,01; ***p< 0,001; students t-test). Error bars indicate SE of three independent experiments in A and B.

References

Audenaert, K., Vanheule, A., Höfte, M., and Haesaert, G. (2014). Deoxynivalenol: A major player in the multifaceted response of Fusarium to its environment. Toxins. 6, 1–19.

Bai, Y., Lan, F., Yang, W., Zhang, F., Yang, K., Li, Z. et al. (2015). sRNA profiling in *Aspergillus flavus* reveals differentially expressed miRNA-like RNAs response to water activity and temperature. *Fungal Genet. Biol*. 81, 113–119.

Baulcombe, D.C. (2013). Small RNA-the Secret of Noble Rot. *Science*. 342(6154), 45–46.

Brandfass, C., and Karlovsky, P. (2008). Upscaled CTAB-based DNA extraction and real-time PCR assays for *Fusarium culmorum* and *F. graminearum* DNA in plant material with reduced sampling error. *Int. J. Mol. Sci*. 9(11), 2306–2321.

Brown, N., Evans, A.J., Mead, A., and Hammond-Kosack, K.E. (2017). A spatial temporal analysis of the *Fusarium graminearum* transcriptome during symptomless and symptomatic wheat infection. *Mol. Plant Pathol.* 18(9), 1295–1312.

Cai, Q., He, B., Kogel, K.H., and Jin, H. (2018). Cross-kingdom RNA trafficking and environmental RNAi — nature's blueprint for modern crop protection strategies. Curr. Opin. Microbiol. 46, 58–64.

Calo, S., Nicolás, F.E., Vila, A., Torres-Martínez, S., and Ruiz-Vázquez, R.M. (2012). Two distinct RNA-dependent RNA polymerases are required for initiation and amplification of RNA silencing in the basal fungus Mucor circinelloides. *Mol. Microbiol*. 83(2), 379-94.

Campo, S., Gilbert, K.B., and Carrington, J.C. (2016). Small RNA-based antiviral defense in the phytopathogenic fungus *Colletotrichum higginsianum*. *PLoS Pathog*. doi: 10.1371/journal.ppat.1005640.

591 Carreras-Villaseñor, N., Esquivel-Naranjo, E.U., Villalobos-Escobedo, J.M., Abreu-Goodger, C., and
592 Herrera-Estrella, A. (2013). The RNAi machinery regulates growth and development in the filamentous
593 fungus *Trichoderma atroviride*. *Mol. Microbiol*. 89(1), 96–112.

594 Cavinder, B., Sikhakolli, U., Fellows, K.M., Trail, F. (2012). Sexual development and ascospore
595 discharge in *Fusarium graminearum*. *J. Vis. Exp*. doi: 10.3791/3895.

596 Chang, SS, Zhang, Z, and Liu, Y. (2012). RNA interference pathways in fungi: mechanisms and
597 functions. *Annu. Rev. Microbiol*. 66, 305–23.

598 Chen, Y, Gao, Q., Huang, M., Liu, Y., Liu, .Z, Liu X., and Ma, Z. (2015). Characterization of RNA
599 silencing components in the plant pathogenic fungus *Fusarium graminearum*. *Sci Rep.* 5, 12500.

600 Cogoni, C, and Macino, G. (1999). Gene silencing in *Neurospora crassa* requires a protein homologous
601 to RNA-dependent RNA polymerase. *Nature*. 399(6732), 166–169.

602 Cuomo, C.A., Güldener, U., Xu, J.R., Trail, F., Turgeon, B.G., Di Pietro A., et al. (2007). The *Fusarium*
603 *graminearum* genome reveals a link between localized polymorphism and pathogen specialization.
604 *Science*. 317(5843), 1400–1402.

605 Dalakouras, A, Wassenegger, M, McMillan, J.N., Cardoza, V., Maegele, I, Dadami, E., Runne, M,
606 Krczal, G., and Wassenegger, M.K. (2016). Induction of silencing in plants by high-pressure spraying
607 of *in vitro*-synthesized small RNAs. *Front. Plant Sci*. doi.org/10.3389/fpls.2016.01327.

608 Dang, Y, Yang, Q, Xue, Z, and Liu, Y. (2011). RNA Interference in Fungi: Pathways, Functions, and
609 Applications. *Eukaryot. Cell*. 10(9), 1148–1155.

610 Dean, R., Van Kan, J.A., Pretorius, Z.A., Hammond-Kosack, K.E., Di Pietro, A., Spanu, P.D., Rudd,
611 J.J., Dickman, M., Kahmann, R., Ellis J., and Foster, G.D. (2012). The top 10 fungal pathogens in
612 molecular plant pathology. *Mol. Plant Pathol*. 13, 414–430.

613 Desjardins, A.E., Hohn, T.M., and McCormick, S.P. (1993). Trichothecene biosynthesis in Fusarium
614 species: Chemistry, genetics and significance. *Microbiol. Rev*. 57(3), 595–604.

615 Dill-Macky, R, and Jones, RK. (2000). The effect of previous crop residues and tillage on Fusarium
616 head blight of wheat. *Plant Dis*. 84, 71–76.

617 Fire, A, Xu, S, Montgomery, MK, Kostas, SA, Driver, SE, and Mello, CC. (1998). Potent and specific
618 genetic interference by double-stranded RNA in *Caenorhabditis elegans*. *Nature*. 391(6669), 806–811.

619 Frandsen, R.J., Nielsen, N.J., Maolanon, N., Sørensen, J.C., Olsson, S., Nielsen, J., and Giese, H. (2006).
620 The biosynthetic pathway for aurofusarin in *Fusarium graminearum* reveals a close link between the
621 naphthoquinones and naphthopyrones. *Mol Microbiol*. 61(4), 1069–1080.

622 Gosman, N., Steed, A., Chandler, E., Thomsett, M., and Nicholson, P. (2010). Evaluation of type I
623 fusarium head blight resistance of wheat using non-deoxynivalenol-producing fungi. *Plant Pathol*.
624 59(1), 147–157.

625 Hallen, H, Huebner, M, Shiu, SH, Guldener, U, and Trail, F. (2007). Gene expression shifts during
626 perithecium development in *Gibberella zeae* (anamorph *Fusarium graminearum*), with particular
627 emphasis on ion transport proteins. *Fungal Genet. Biol*. 44(11), 1146–1156.

628 Hammond, S.M. (2005). Dicing and slicing: the core machinery of the RNA interference pathway. *FEBS*
629 *Lett*. 579(26), 5822-5829.

630 Harris, L.J, Balcerzak, M., Johnston, A., Schneiderman, D., and Ouellet, T. (2016). Host-preferential
631 *Fusarium graminearum* gene expression during infection of wheat, barley, and maize. *Fungal Biol*. 120
632 (1), 111–123.

633 Ilgen, P., Hadeler, B., Maier, F.J., and Schäfer, W. (2009). Developing kernel and rachis node induce
634 the trichothecene pathway of *Fusarium graminearum* during wheat head infection. *Mol. Plant Microbe*
635 *Interact*. 22(8), 899–908.

636 Jansen, C., von Wettstein, D., Schäfer, W., Kogel, K.H., Felk, F., and Maier, F.J. (2005). Infection
637 patterns in barley and wheat spikes inoculated with wild type and trichodiene synthase gene disrupted
638 *Fusarium graminearum. Proc. Natl. Acad. Sci USA.* 102 (46), 16892–16897.

639 Kim, H.K., Jo, S.M., Kim, G.Y., Kim D.W., Kim, Y.K., and Yun, S.H. (2015). A large-scale functional
640 analysis of putative target genes of mating-type loci provides insight into the regulation of sexual
641 development of the cereal pathogen *Fusarium graminearum*. *PLoS Genet*. 3;11(9):e1005486.

642 Klittich, C.J.R., and Leslie, J.F. (1988). Nitrate reduction mutants of *Fusarium moniliforme* (*Gibberella*
643 *fujikuroi*). *Genetics*. 118(3), 417–423.

644 Koch, A., Biedenkopf, D., Furch, A., Weber, L., Rossbach O., Abdellatef E., Linicus, L., Johannsmeier,
645 J., Jelonek, L., Goesmann, A., Cardoza V., McMillan, J., Mentzel, T., and Kogel, K.-H. (2016). An
646 RNAi-Based Control of *Fusarium graminearum* infections through spraying of Long dsRNAs involves
647 a plant passage and is controlled by the fungal silencing machinery. *PLoS Pathog.*
648 doi:10.1371/journal.ppat.1005901.

649 Koch, A., and Kogel, K.H. (2014). New wind in the sails: improving the agronomic value of crop plants
650 through RNAi-mediated gene silencing. *Plant Biotechnol. J*. 12(7), 821-31.

651 Koch, A., Kumar, N., Weber, L., Keller, H., Imani, J., and Kogel, K.H. (2013). Host-induced gene
652 silencing of cytochrome P450 lanosterol C14α-demethylase–encoding genes confers strong resistance
653 to Fusarium species. *Proc. Natl. Acad. Sci. USA.* 110(48), 19324–19329.

654 Koch, A., Stein, E., and Kogel, K.-H. (2018). RNA-based disease control as a complementary measure
655 to fight Fusarium fungi through silencing of the Azole target cytochrome P450 lanosterol C-14 α-
656 demethylase. *Eu. J Plant Pathol.* 152(4), 1003–1010.

657 Kusch, S., Frantzeskakis, L., Thieron, H., and Panstruga, R. (2018). Small RNAs from cereal powdery
658 mildew pathogens may target host plant genes. *Fungal Biol*. 122(11), 1050–1063.

659 Lau, S.K., Tse, H., Chan, J.S., Zhou, A.C., Curreem, S.O., Lau, C.C., Yuen, K.Y., and Woo, P.C. (2013).
660 Proteome profiling of the dimorphic fungus *Penicillium marneffei* extracellular proteins and
661 identification of glyceraldehyde-3-phosphate dehydrogenase as an important adhesion factor for
662 conidial attachment. *FEBS J*. 280(24), 6613–26.

663 Leslie, J.F., Summerell, B.A. (2006) The Fusarium laboratory manual. Blackwell Professional, Ames,
664 IA, USA; ISBN: 978-0-813-81919-8.

665 Livak, K.J., Schmittgen, T.D. (2001). Analysis of relative gene expression data using real-time
666 quantitative PCR and the 2ΔΔC(T). *Methods*. 25(4), 402–408.

667 Maldonado-Ramirez, S.L., Schmale, D.G., Jr Shields, E.J., and Bergstrom, G.C. (2005). The relative
668 abundance of viable spores of *Gibberella zeae* in the planetary boundary layer suggests the role of long-
669 distance transport in regional epidemics of Fusarium head blight. *Agric. For. Meteorol*. 132, 20–27.

670 Malz, S., Grell, M.N., Thrane, C., Maier, F.J., Rosager, P., Felk, A., Albertsen, K.S., Salomon, S., Bohn
671 L., Schäfer, W., and Giese, H. (2005). Identification of a gene cluster responsible for the biosynthesis
672 of aurofusarin in the *Fusarium graminearum* species complex. *Fungal Genet. Biol*. 42(5), 420–33.

673 McLoughlin, A.G., Wytinck, N., Walker, P.L., Girard, I.J., Rashid, K.Y., de Kievit, T., Dilantha, W.G.
674 Fernando, Whyard, S. and Belmonte, M.F. (2018) 1Identification and application of exogenous dsRNA
675 confers plant protection against *Sclerotinia sclerotiorum* and *Botrytis cinerea*. *Sci. Rep.* 8, 7320.

676 Medentsev, A.G., Kotik, A.N., Trufanova, V.A., and Akimenko, V.K. (1993). Identification of
677 aurofusarin in *Fusarium graminearum* isolates, causing a syndrome of worsening of egg quality in
678 chickens. *Prikl Biokhim Mikrobiol*. 29(4), 542–546.

679 Mello, C.C., and Conte, D, Jr. (2004). Revealing the world of RNA interference. *Nature* 431(7006),
680 338–342.

Meng, H, Wang, Z, Wang, Y, Zhu, H., and Huang, B. (2017). Dicer and Argonaute genes involved in RNA interference in the entomopathogenic fungus *Metarhizium robertsii*. *Appl. Environ. Microbiol*. 83(7) pii: e03230-16. .

Nguyen, Q., Iritani, A., Ohkita, S., Vu, B.V., Yokoya, K., Matsubara, A., Ikeda, K.I., Suzuki, N., Nakayashiki, H. (2018). A fungal Argonaute interferes with RNA interference. *Nucleic Acids Res*. 46(5), 2495–2508.

Nowara, D., Gay, A., Lacomme, C., Shaw, J., Ridout, C., Douchkov, D., Hensel, G., Kumlehn, J., and Schweizer, P. (2010). HIGS: Host-induced gene silencing in the obligate biotrophic fungal pathogen *Blumeria graminis*. *Plant Cell*. 22, 3130–3141.

Qi, W., Kwon, C., and Trail, F. (2006). Microarray analysis of transcript accumulation during perithecium development in *Gibberella zeae* (anamorph *Fusarium graminearum*). *Mol. Genet. Genomics* 276(1), 87–100.

Raman, V., Simon, S.A., Demirci, F., Nakano, M., Meyers, B.C., and Donofrio, N.M. (2017) Small RNA functions are required for growth and development of *Magnaporthe oryzae*. *Mol. Plant Microbe Interact*. 30(7), 517–530.

Romano, N., and Macino, G. (1992). Quelling: transient inactivation of gene expression in *Neurospora crassa* by transformation with homologous sequences. *Mol. Microbiol*. 6(22), 3343-53.

Segers, G.C., Zhan,g X., Deng, F., Sun, Q., and Nuss, D.L. (2007). Evidence that RNA silencing functions as an antiviral defense mechanism in fungi. *Proc. Natl. Acad. Sci.* USA. 104(31), 12902–12906.

Shiu, P.K., Raju, N.B., Zickler, D., and Metzenberg, R.L. (2001). Meiotic silencing by unpaired DNA. *Cell*. 107(7), 905–916.

Son, H., Min, K., Lee, J., Raju, N.B., and Lee, Y.W. (2011). Meiotic silencing in the homothallic fungus *Gibberella zeae*. *Fungal Biol*. 115(12), 1290-302.

Son, H., Park, A.R., Lim, J.Y., Shin, C., and Lee, Y.W. (2017). Genome-wide exonic small interference RNA-mediated gene silencing regulates sexual reproduction in the homothallic fungus *Fusarium graminearum*. *PLoS Genet*. doi.org/10.1371/journal.pgen.1006595.

Song, M.S., and Rossi, J.J. (2017). Molecular mechanisms of Dicer: endonuclease and enzymatic activity. *Biochem J*. 474(10), 1603–1618.

Sulyok, M., Berthiller, F., Krska, R., and Schuhmacher, R. (2006). Development and validation of a liquid chromatography/tandem mass spectrometric method for the determination of 39 mycotoxins in wheat and maize. *Rapid Commun. Mass Spectrom.* 20(18), 2649–2659.

Torres-Martínez, S., and Ruiz-Vázquez, R.M. (2017). The RNAi universe in fungi: A varied landscape of small RNAs and biological functions. *Annu. Rev. Microbiol*. 71, 371–391.

Trail, F., and Common, R. (2000). Perithecial development by *Gibberella zeae*: a light microscopy study. *Mycologia*. 92, 130–138.

Urban, M., King, R., Hassani-Pak, K., and Hammond-Kosack, K.E. (2015). Whole-genome analysis of *Fusarium graminearum* insertional mutants identifies virulence associated genes and unmasks untagged chromosomal deletions. *BMC Genomics*. 16, 261.

Vervliet, G., Holsters, M., Teuchy, H., Van Montagu, M., and Schell, J. (1975). Characterization of different plaque-forming and defective temperate phages in Agrobacterium strains. *J. Gen. Virol*. 26, 33–48.

Wang, S., Li P., Zhang, J., Qiu, D., and Guoa, L. (2016a). Generation of a high resolution map of sRNAs from *Fusarium graminearum* and analysis of responses to viral infection. *Scientific Reports*. 6, 26151.

Wang, M., Weiberg, A., Lin, F.M., Thomma, B.P., Huang, H.D., and Jin, H. (2016b). Bidirectional cross-kingdom RNAi and fungal uptake of external RNAs confer plant protection. *Nature Plants 2*, 16151.

Weiberg, A., Wang, M., Lin, F.-M., Zhao, H., Zhang, Z., et al. (2013). Fungal small RNAs suppress plant immunity by hijacking host RNA interference pathways. *Science*. 342(6154), 118–23 .

Yun, Y., Liu Z., Yin, Y., Jiang, J., Chen, Y., Xu, J.R., and Ma, Z. (2015). Functional analysis of the *Fusarium graminearum* phosphatome. *New Phytol*. 207(1), 119–134.

Zanini, S., Šečić, E., Jelonek, L., Kogel, K.-H. (2018). A bioinformatics pipeline for the analysis and target prediction of RNA effectors in bidirectional communication during plant-microbe interactions. *Front. Plant Sci*. doi: 10.3389/fpls.2018.01212.

Zanini, S., Šečić, E., Busche, T., Kalinowski, T., Kogel, K.-H. (2019). Discovery of interaction-related sRNAs and their targets in the *Brachypodium distachyon* and *Magnaporthe oryzae* pathosystem. BioRxiv doi: https://doi.org/10.1101/631945.

Zeng, W., Wang, J., Wang, Y., Lin, J., Fu, Y., Xie, J., Jiang, D., Chen, T., Liu H., and Cheng, J. (2018). Dicer-like proteins regulate sexual development via the biogenesis of perithecium-specific microRNAs in a plant pathogenic fungus *Fusarium graminearum*. *Frontiers Microb.* doi: 10.3389/fmicb.2018.00818.

Zhang, H., Xia, R., Meyers, B.C., Walbot, V. (2015). Evolution, functions, and mysteries of plant ARGONAUTE proteins. *Curr. Opin. Plant Biol*. 27, 84–90.

746 **Table 1**: RNAi pathway genes of *Fusarium graminearum* (*Fg*) as identified from
747 www.Broadinstitute.org and used in this study.
748

RNAi proteins in *Neurospora crassa*	**Homologs in *Fg***	**aa identity (%)**	**Fusarium gene ID**	**Gene function in *Fg***
DICER 1	*Fg*DCL1	43%	FGSG_09025	Antiviral defence (Wang et al., 2016a). Minor role in processing of exogenous dsRNA, hpRNA or pre-milRNA in mycelium (Chen et al., 2015). Major role in sex-specific RNAi pathway: Production of regulatory sRNAs. Required for ascospore production (Son et al., 2017).
DICER 2	*Fg*DCL2	35%	FGSG_04408	Processing of exogenous dsRNA, hpRNA and pre-milRNA in mycelium (Chen et al., 2015). Partially shared DCL-1 role in production of regulatory sRNAs in the sexual stage (Son et al., 2017).
ARGONAUTE 1 (syn. Quelling defective 2)	*Fg*AGO1	59%	FGSG_08752	Major component in the RISC during quelling (Chen et al., 2015).
ARGONAUTE 2 (syn. Suppressor of meiotic silencing 2, SMS2)	*Fg*AGO2	43%	FGSG_00348	Minor role in binding siRNA derived from exogenous dsRNA, hpRNA or pre-milRNA in mycelium (Chen et al., 2015). Major role in sex-specific RNAi pathway; required for ascospore production (Son et al., 2017).
RNA-DEPENDENT RNA POLYMERASE (syn. Quelling defective 1)	*Fg*RdRP1	38%	FGSG_06504	Maybe associated with secondary sRNA production (Chen et al., 2015).
	*Fg*RdRP4	33%	FGSG_04619	Maybe associated with secondary sRNA production (Chen et al., 2015).
RNA-DEPENDENT RNA POLYMERASE (syn. Suppressor of ascus dominance, SAD1)	*Fg*RdRp2	42%	FGSG_08716	Maybe associated with secondary sRNA production (Chen et al., 2015).
	*Fg*RdRp5	29 %	FGSG_09076	Roles in the antiviral defence. Maybe associated with secondary sRNA production (Chen et al., 2015).
RNA-DEPENDENT RNA POLYMERASE (RRP3)	*Fg*RdRP3	47%	FGSG_01582	Maybe associated with secondary sRNA production (Chen et al., 2015).
QDE2-INTERACTING PROTEIN	*Fg*QIP	32%	FGSG_06722	The homolog has been identified in (Chen et al., 2015), but not yet studied in depth.
RecQ HELICASE QDE3	*Fg*QDE3	46%	FGSG_00551	not studied.

749

Table 2: Function of *Fusarium graminearum* RNAi mutants in various developmental and pathogenic processes.

Fungal strain	[1]aurofusarin pigment	[2]conidiation	[2]conidial germination	ascospore discharge	ascospore germination	[3]spike infection	rDON	[4]SIGS
IFA WT	+	+	+	+	+	+	+	+
Δdcl1	-	--	(-)	--	(+)	--	(-)	-
Δdcl2	-	-	(-)	-	+	++	(-)	-
Δago1	++	--	--	-	(+)	+	--	(+)
Δago2	+	(+)	--	--	+	-	--	(+)
Δrdrp1	-	(+)	(-)	--	+	+	+	(+)
Δrdrp2	++	--	+	--	+	+	--	nd
Δrdrp3	++	--	(-)	+	--	+	--	nd
Δrdrp4	++	-	--	+	--	+	--	nd
Δqde3	-	--	+	--	+	+	+	+
Δqip	-	--	+	-	(+)	+	+	--
Δdcl1 Δdcl2	nd	nd	nd	nd	nd	nd	nd	--
PH1	nd	nd	nd	nd	nd	nd	nd	+

[1]In liquid PEG medium under day light conditions; [2]Dimmed light (2 µmol m^{-2} s^{-1}), liquid SN cultures; [3]At 9 dpi (not on 13 dpi); [4]On barley leaves, 20 ng μL^{-1} CYP3RNA; conclusion from two independent validation assays.

Table 3: Trichothecenes produced by RNAi mutants in infected wheat kernels at 13 dpi.

Samples	**ng *Fg* DNA /mg seed d.w.**	**DON [mg/kg seed]**	**DON/DNA**	**[1]A-DON [mg/kg seed]**	**[2]A-DON/DON x1000**
Mock (without *Fg*)	0	0.00	0	0	0
Δago1	0.84	12.7	15.2	0.45	36
Δago2	1.28	32.3	25.2	1.04	32
Δdcl1	2.86	61.9	21.6	1.87	30
Δdcl2	2.03	56.6	27.9	1.89	33
Δrdrp1	4.84	86.7	17.9	3.51	40
Δrdrp2	0.95	16.9	17.8	0.43	25
Δrdrp3	0.78	12.3	15.6	0.35	29
Δrdrp4	0.47	4.90	10.3	0.15	31
Δqip	2.53	68.7	27.2	2.87	42
Δqde3	4.33	82.3	19.0	3.91	47
IFA WT	2.18	78.3	35.9	2.58	33

DON, deoxynivalenol; A-DON, acetyldeoxynivalenol.

[1] 3A-DON (3-acetyldeoxynivalenol) and 15A-DON (15-acetyldeoxynivalenol) were measured

[2] Ratio of concentrations of A-DON and DON, multiplied by 1000

Supplement data:

Supplement figures

Figure S1:
Schematic representation of the gene replacement strategy used for *F. graminearum* transformation. Yellow box: the target gene that has to be replaced by KO; dark green box: selection marker gene, in this case the antibiotic resistance gene (*hygromycin B phosphotransferase* of *E. coli*, hph). Blue arrow: Homologous recombination sequences, typically ~1 kb long; Black arrows: template area for primers binding used for transformants genotyping. PgpdA: Promoter region of the *Glyceraldehyde-3-phosphate dehydrogenase* gene of *Aspergillus nidulans*; TtrpC: termination region of the *Aspergillus nidulans trpC* gene.

Fig. S2. Compromised expression of deleted RNAi genes in *F. graminearum* knockout (KO) mutants. Expression of the targeted genes in respective Fusarium mutants. Transcript levels were analyzed by qRT-PCR from five-day-old PEG liquid cultures and transcript quantified by normalization to Fusarium *β-TUBULIN* (*FgTub*) or *ELONGATION FACTOR A* (*FgEF1a*) and comparison to IFA WT.

Figure S3. Colony morphology and growth of RNAi KO mutants. Fusarium mutants and wt IFA WT were grown for 5 days on solid (A) PDA (potato dextrose agar), (B) SN (synthetic nutrient), (C) CM (Aspergillus complete medium) and in liquid PEG medium without hygromycin. The mutants showed differences in pigmentation as follows: *Δago1*, *Δrdrp2*, *Δrdrp3* and *Δrdrp4* darker pigmentation; *Δdcl1*, *Δdcl2* and *Δrdrp1* reduced pigmentation compared to IFA WT.

Fig. S4. Infection of wheat spikes with *F. graminearum* RNAi mutants and IFA WT. Thousand grain weight (TGW) of infected wheat spikes. Mock control: Kernels treated with 0.002% Tween 20; mature kernels: completely mature Apogee kernels.

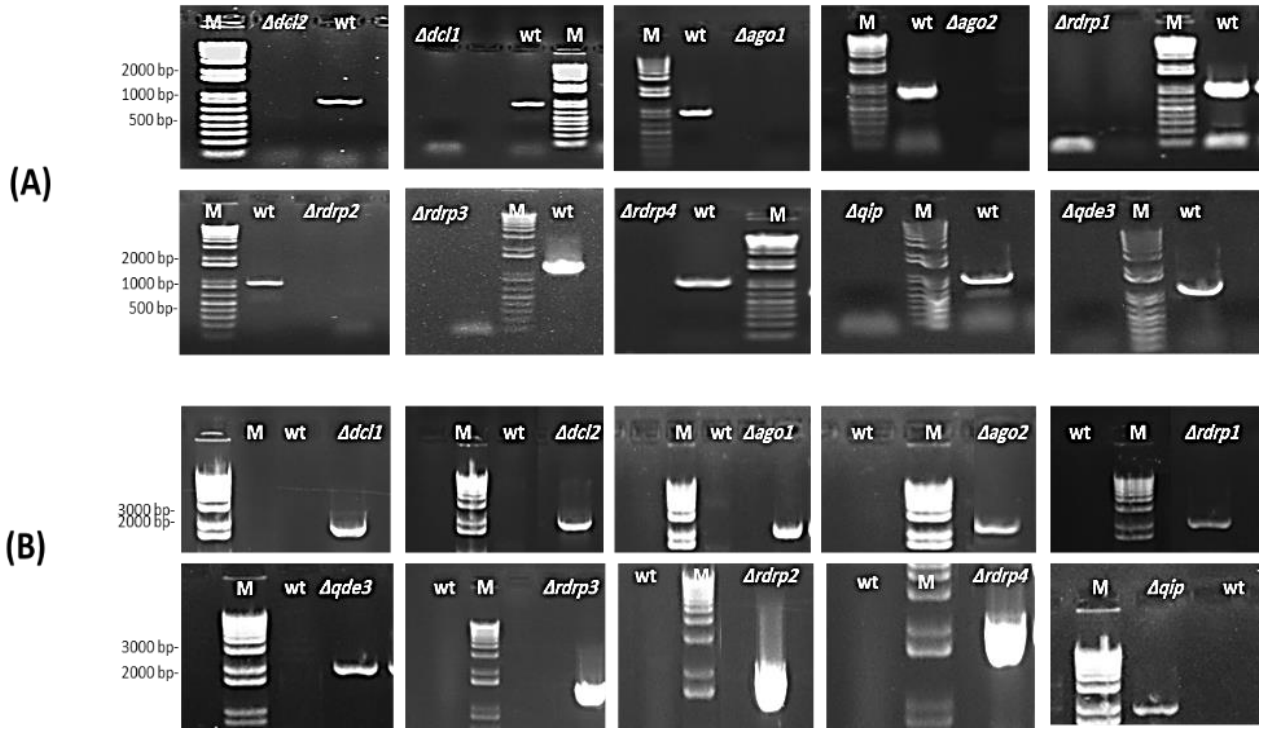
(A)
M
Δdcl2
wt
Δdcl1
wt
M
M
wt
Δago1
M
wt
Δago2
Δrdrp1
M
wt
2000 bp-
1000 bp-
500 bp-
M
wt
Δrdrp2
Δrdrp3
M
wt
Δrdrp4
wt
M
Δqip
M
wt
Δqde3
M
wt
2000 bp-
1000 bp-
500 bp-
(B)
M
wt
Δdcl1
M
wt
Δdcl2
M
wt
Δago1
wt
M
Δago2
wt
M
Δrdrp1
3000 bp-
2000 bp-
M
wt
Δqde3
wt
M
Δrdrp3
wt
M
Δrdrp2
wt
M
Δrdrp4
M
Δqip
wt
3000 bp-
2000 bp-

Fig. 1

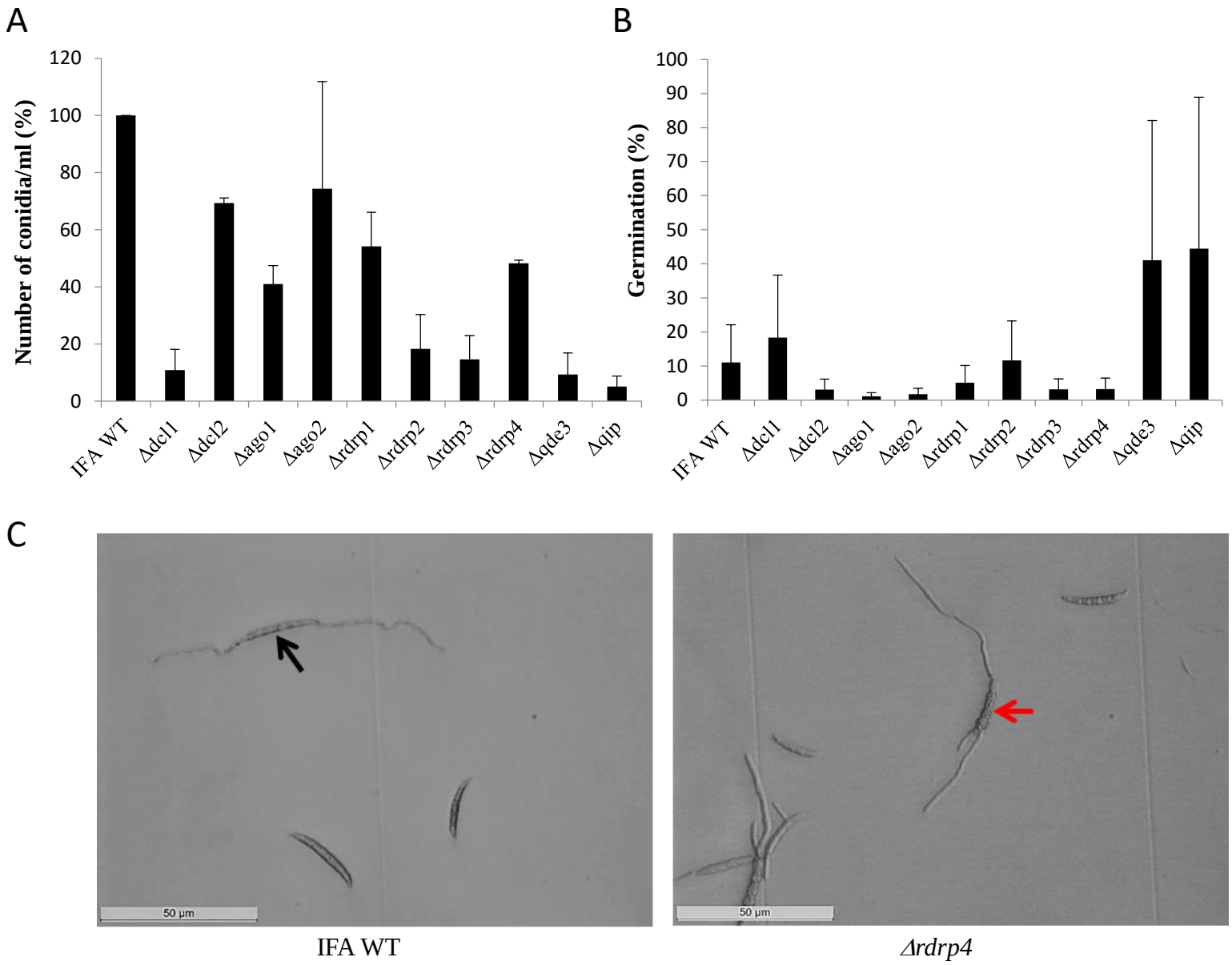
A
Number of conidia/ml (%)
120
100
80
60
40
20
0
IFA WT
Δdcl1
Δdcl2
Δago1
Δago2
Δrdrp1
Δrdrp2
Δrdrp3
Δrdrp4
Δqde3
Δqip
B
Germination (%)
100
90
80
70
60
50
40
30
20
10
0
IFA WT
Δdcl1
Δdcl2
Δago1
Δago2
Δrdrp1
Δrdrp2
Δrdrp3
Δrdrp4
Δqde3
Δqip
C
50 µm
50 µm
IFA WT
Δrdrp4

Fig. 2

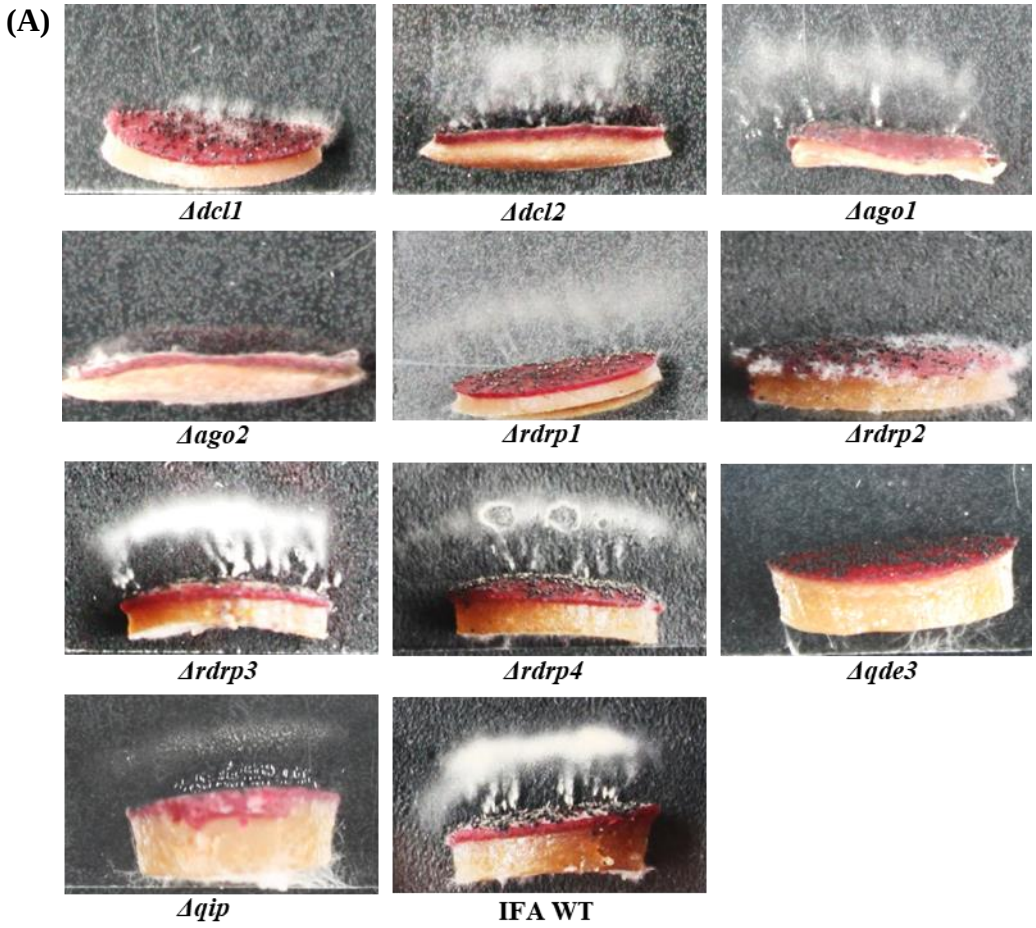
(A)
Δdcl1
Δdcl2
Δago1
Δago2
Δrdrp1
Δrdrp2
Δrdrp3
Δrdrp4
Δqde3
Δqip
IFA WT

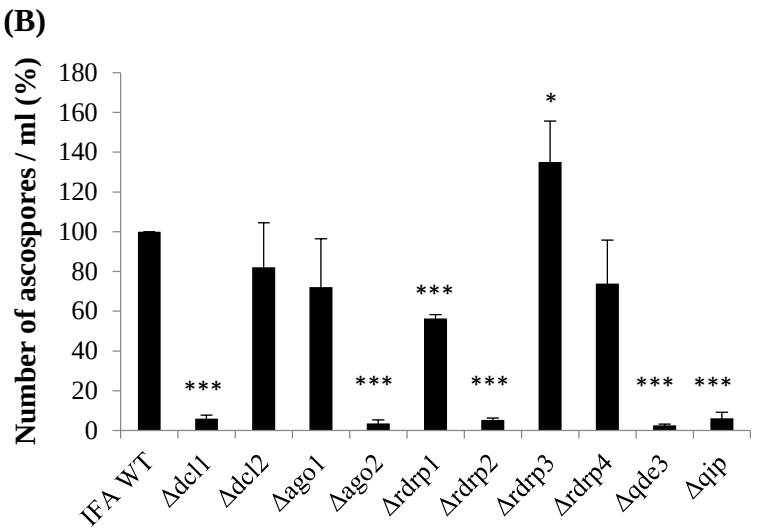
(B)
Number of ascospores / ml (%)
180
160
140
120
100
80
60
40
20
0
***
***
***
***
*
***
***
IFA WT
Δdcl1
Δdcl2
Δago1
Δago2
Δrdrp1
Δrdrp2
Δrdrp3
Δrdrp4
Δqde3
Δqip

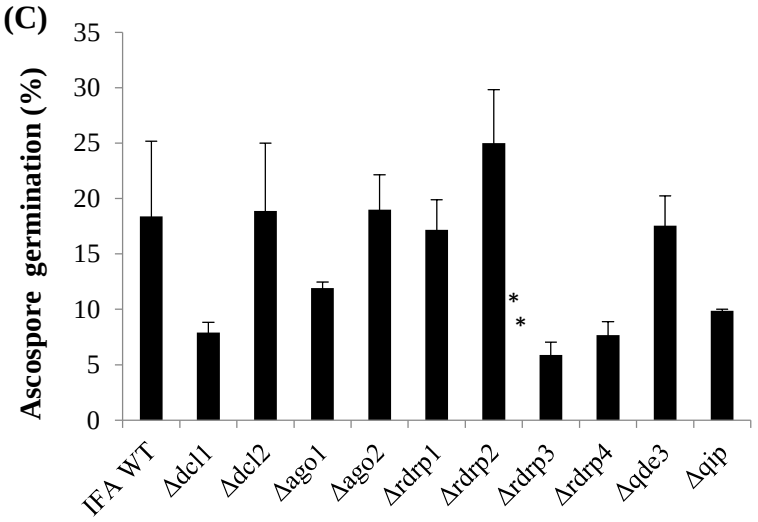
(C)
Ascospore germination (%)
35
30
25
20
15
10
5
0
*
*
IFA WT
Δdcl1
Δdcl2
Δago1
Δago2
Δrdrp1
Δrdrp2
Δrdrp3
Δrdrp4
Δqde3
Δqip

Fig. 3

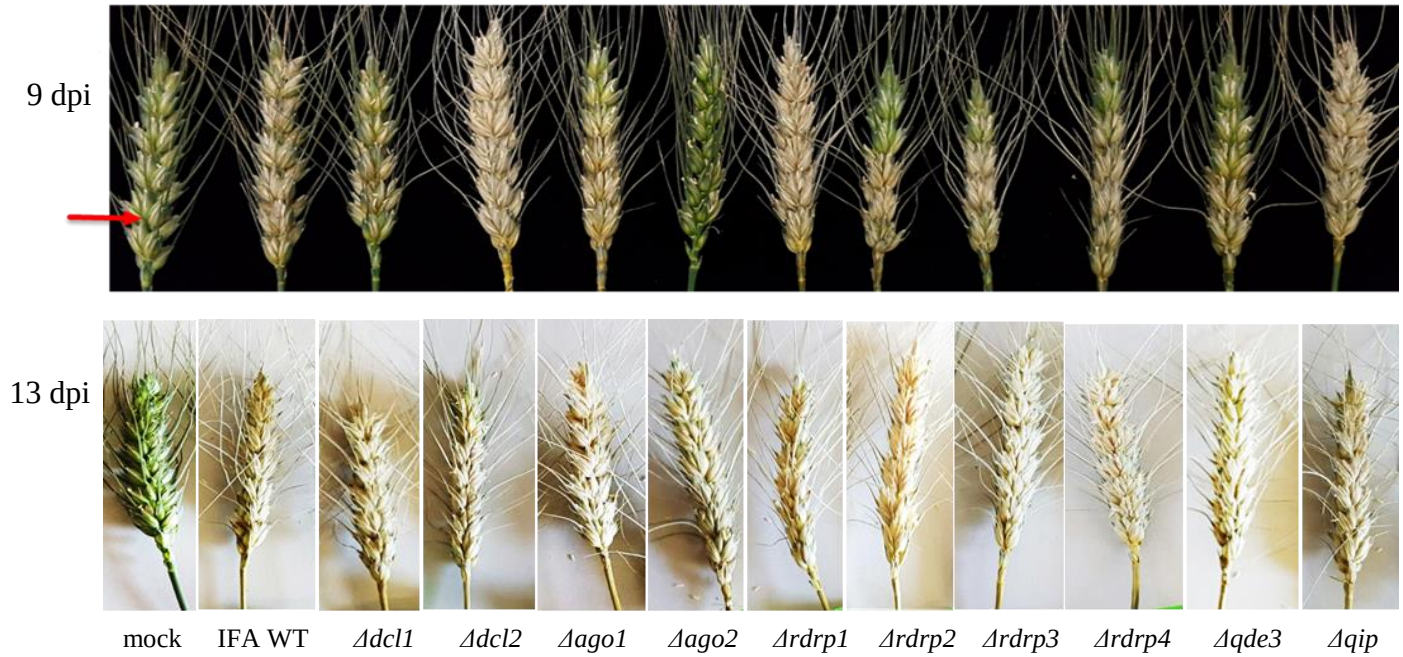
9 dpi
13 dpi
mock
IFA WT
Δdcl1
Δdcl2
Δago1
Δago2
Δrdrp1
Δrdrp2
Δrdrp3
Δrdrp4
Δqde3
Δqip

Fig. 4

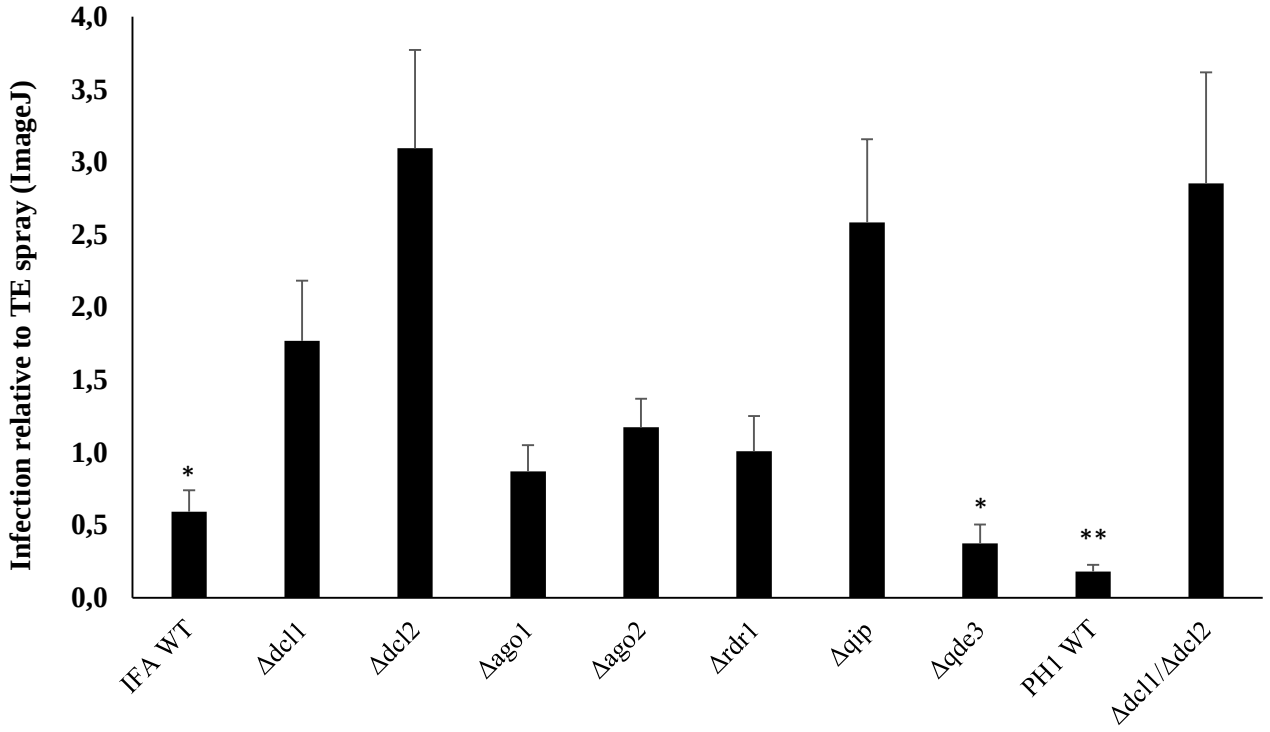
Infection relative to TE spray (ImageJ)
4,0
3,5
3,0
2,5
2,0
1,5
1,0
0,5
0,0
*
*
**
IFA WT
Δdcl1
Δdcl2
Δago1
Δago2
Δrdr1
Δqip
Δqde3
PH1 WT
Δdcl1/Δdcl2

Fig. 5A

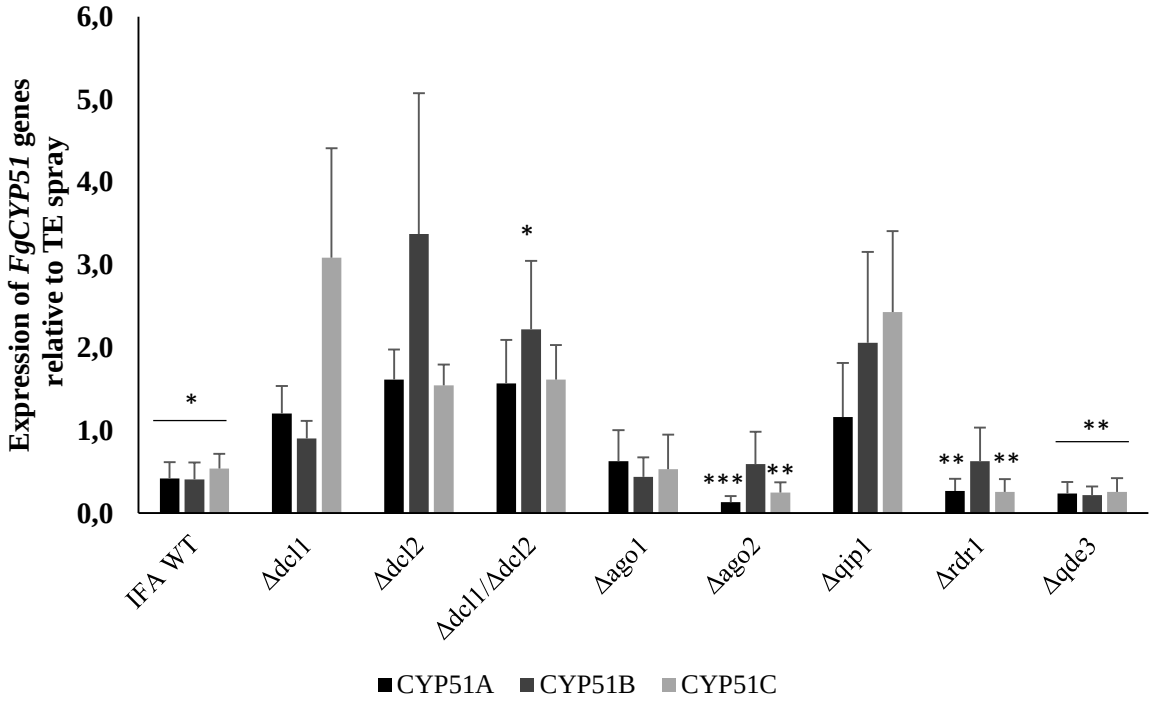
Expression of FgCYP51 genes relative to TE spray
6,0
5,0
4,0
3,0
2,0
1,0
0,0
*
*
***
**
**
**
**
IFA WT
Δdcl1
Δdcl2
Δdcl1/Δdcl2
Δago1
Δago2
Δqip1
Δrdr1
Δqde3
CYP51A
CYP51B
CYP51C

Fig. 5B